
LATTICE DYNAMICS
AND PHASE TRANSITIONS

Statistical Mechanics of Cation Ordering and Lattice Dynamics of $\text{PbZr}_x\text{Ti}_{1-x}\text{O}_3$ Solid Solutions

V. I. Zinenko and S. N. Sofronova

Kirensky Institute of Physics, Siberian Division, Russian Academy of Sciences,
Akademgorodok, Krasnoyarsk, 660036 Russia

e-mail: zvi@iph.krasn.ru

Received August 28, 2003

Abstract—An effective Hamiltonian for Zr–Ti cation ordering in $\text{PbZr}_x\text{Ti}_{1-x}\text{O}_3$ solid solutions is written out. To determine the parameters of the effective Hamiltonian, a nonempirical calculation is performed within an ionic-crystal model taking into account the deformation and dipole and quadrupole polarizabilities of ions. The thermodynamic properties of cation ordering are studied using the Monte Carlo method. The calculated phase transition temperatures (180 and 250 K for the concentrations $x = 1/3$ and $1/2$, respectively) are much lower than the melting temperature of the compound under study. At such temperatures, the ordering kinetics is frozen and, in reality, the phase transition to the ordered phase does not occur, in agreement with experimental observations. Within the same ionic-crystal model, we calculated the high-frequency permittivity, Born dynamic charges, and the lattice vibration spectrum for a completely disordered phase and certain ordered phases. It is shown that soft vibration modes, including ferroelectric ones, exist in the lattice vibration spectrum of both the completely disordered and the ordered phases. © 2004 MAIK “Nauka/Interperiodica”.

1. INTRODUCTION

Solid solutions of lead titanate and lead zirconate $\text{PbZr}_x\text{Ti}_{1-x}\text{O}_3$ (PZT) have been attracting research attention for many decades; a great number of experimental and theoretical studies have dealt with their physical properties. The PZT system has a complicated phase diagram and a number of interesting properties in terms of both theory and application (in particular, high values of the piezoelectric constants).

At high temperatures, PZT has a perovskite structure. As the temperature is decreased, this compound exhibits structural phase transitions to a rhombohedral, an orthorhombic, or a monoclinic phase with ferroelectric or antiferroelectric ordering, depending on the Zr/Ti content ratio (see, e.g., [1] and references therein). Phase transitions related to the ordering of tetravalent zirconium and titanium cations have not been observed experimentally at any concentration or temperature; however, there are experimental indications that, in the samples under study, there exist small regions with an ordered distribution of titanium and zirconium ions over the lattice sites [2]. Apparently, the presence of such ordered regions has a significant effect on lattice instability with respect to ferroelectric, antiferroelectric, and rotational distortions [3]. The properties of the solid solutions, in particular, the energies of different structures [4], some lattice vibration frequencies in the distorted phases [3], and Born effective charges in the disordered and ordered phases [5–8], were studied by performing *ab initio* calculations using different approaches in combination with the density functional method. However, the phase transitions

related to ordering of titanium and zirconium ions over the lattice sites were not discussed in the papers mentioned above; it was only noted that the energy of such ordering is small, because the valences of ions randomly distributed over the perovskite structure are equal.

In this paper, we perform a nonempirical calculation within an ionic-crystal model including the deformation and dipole and quadrupole polarizabilities of ions to study phase transitions related to ordering of titanium and zirconium ions and determine the entire vibration frequency spectrum of the disordered phase, the vibration frequencies at $q = 0$ for the ordered phases, the Born effective charges, and the high-frequency permittivity.

In Section 2, we introduce an effective Hamiltonian describing phase transitions of the order–disorder type in a model two-component Zr/Ti alloy. The parameters of the effective Hamiltonian, in which interactions within the first three coordination shells are taken into account, are determined by calculating the total energy of the crystal in different ordered phases. At certain values of the parameters of the effective Hamiltonian, using the Monte Carlo method, we study the thermodynamic properties of the system, namely, the phase transition temperatures and the temperature dependences of the heat capacity and of the long-range and short-range order parameters.

In Section 3, in the virtual-crystal approximation for different values of the Zr/Ti content ratio, we calculate the permittivity, Born effective charges, and the entire lattice vibration spectrum of the cubic phase of the dis-

ordered crystal for different concentrations x . Analogous calculations are also carried out for certain ordered phases of $\text{PbZr}_x\text{Ti}_{1-x}\text{O}_3$ with $x = 1/3$ and $1/2$; however, for brevity, we present here only the vibration frequencies at the center of the Brillouin zone.

Finally, in Section 4, we summarize the results of the study.

2. STATISTICAL MECHANICS OF B -CATION ORDERING

To describe phase transitions related to B -cation ordering in $\text{PbZr}_x\text{Ti}_{1-x}\text{O}_3$ solid solutions, we use the effective-Hamiltonian method in which only the degrees of freedom related to positional disorder of titanium and zirconium atoms at the sites of the crystal lattice (the b positions in the O_h space group) are taken into account. In this case, the problem of B -cation ordering in $AB'B''\text{O}_3$ solid solutions is equivalent to the problem of ordering in a two-component alloy and we can use a model based on the assumption that the atoms of a solution are placed at the sites of a certain rigid crystal lattice [9]. The configuration energy of the solution is expressed as the sum of all interatomic pair interaction potentials. In this model, the Hamiltonian of the system can be written as

$$H = \frac{1}{2} \sum_{k,j} [v_{B'B'}(\mathbf{r}_k, \mathbf{r}_j) n_k^{B'} n_j^{B'} + v_{B''B''}(\mathbf{r}_k, \mathbf{r}_j) n_k^{B''} n_j^{B''} + 2v_{B'B''}(\mathbf{r}_k, \mathbf{r}_j) n_k^{B'} n_j^{B''}] - \sum_j [n_j^{B'} \mu_{B'}(\mathbf{r}_j) + n_j^{B''} \mu_{B''}(\mathbf{r}_j)] + H_0, \quad (1)$$

where $v_{B'B'}$, $v_{B''B''}$, and $v_{B'B''}$ are the pair interaction potentials between B' atoms, between B'' atoms, and between B' and B'' atoms, respectively, at lattice sites \mathbf{r}_k and \mathbf{r}_j and $\mu_{B'}$ and $\mu_{B''}$ are the chemical potentials of the cations B' and B'' . The quantities $n_j^{B'}$ and $n_j^{B''}$ are random functions defined as follows: if site j is occupied by a B' atom, then $n_j^{B'} = 1$ and $n_j^{B''} = 0$, and if site j is occupied by a B'' atom, then $n_j^{B'} = 0$ and $n_j^{B''} = 1$. The quantities $n_j^{B'}$ and $n_j^{B''}$ satisfy the relation $n_j^{B'} + n_j^{B''} = 1$. Using this relation, we can rewrite Eq. (1) as [9]

$$H = \frac{1}{2} \sum_{k,j} v(\mathbf{r}_k, \mathbf{r}_j) n_k^{B'} n_j^{B''} - \mu \sum_j n_j^{B'} + H_0, \quad (2)$$

where

$$v(\mathbf{r}_k, \mathbf{r}_j) = v_{B'B'}(\mathbf{r}_k, \mathbf{r}_j) + v_{B''B''}(\mathbf{r}_k, \mathbf{r}_j) - 2v_{B'B''}(\mathbf{r}_k, \mathbf{r}_j)$$

is the effective interaction constant and

$$\mu = \mu_{B'}(\mathbf{r}_j) - \mu_{B''}(\mathbf{r}_j) + \sum_{i,k} (v_{B'B'}(\mathbf{r}_k, \mathbf{r}_j) - v_{B''B''}(\mathbf{r}_k, \mathbf{r}_j))$$

is the chemical potential of the system.

The effective interaction constants are evaluated by performing a nonempirical calculation of the total energy of the crystal in the Gordon–Kim model with inclusion of the dipole and quadrupole polarizabilities of ions [10, 11]. The total energy is

$$E = E_s + E_p + E_q + E_{pq} + E_{\text{self}}, \quad (3)$$

where

$$E_s = -\frac{1}{2} \sum_{i,j=1}^{N_a} Z_i C_{ij}^{(0)} Z_j + \sum_{i,j=1}^{N_a} \Phi_{ij}^{(00)}(V_i, V_j, |\mathbf{R}_i - \mathbf{R}_j|), \quad (4)$$

$$E_p = \frac{1}{2} \sum_{i,j=1}^{N_a} \sum_{\alpha,\beta=1}^3 P_i^\alpha \left(\frac{\delta_{ij}}{-\alpha_i^\beta(V_i)} + \Phi_{ij,\alpha\beta}^{(11)}(V_i, V_j, |\mathbf{R}_i - \mathbf{R}_j|) - C_{ij,\alpha\beta}^{(2)} \right) P_j^\beta \quad (5)$$

$$+ \sum_{i,j=1}^{N_a} \sum_{\alpha=1}^3 P_i^\alpha (\Phi_{ij,\alpha}^{(10)}(V_i, V_j, |\mathbf{R}_i - \mathbf{R}_j|) - C_{ij,\alpha}^{(1)} Z_j),$$

$$E_{qp} = \frac{1}{2} \sum_{i,j=1}^{N_a} \sum_{\alpha,\beta,\gamma,\delta=1}^3 q_i^{\alpha\beta} \left[\frac{\delta_{ij}}{-\alpha_i^\beta(V_i)} - \frac{1}{36} (\Phi_{ij,\alpha\beta\gamma\delta}^{(22)}(V_i, V_j, |\mathbf{R}_i - \mathbf{R}_j|) - C_{ij,\alpha\beta\gamma\delta}^{(4)}) \right] q_j^{\gamma\delta} \quad (6)$$

$$- \frac{1}{6} \sum_{i,j=1}^{N_a} \sum_{\alpha,\beta=1}^3 q_i^{\alpha\beta} (\Phi_{ij,\alpha\beta}^{(20)}(V_i, V_j, |\mathbf{R}_i - \mathbf{R}_j|) - C_{ij,\alpha\beta}^{(2)} Z_j),$$

$$E_q = -\frac{1}{6} \sum_{i,j=1}^{N_a} \sum_{\alpha,\beta,\gamma=1}^3 q_i^{\alpha\beta} (\Phi_{ij,\alpha\beta\gamma}^{(21)}(V_i, V_j, |\mathbf{R}_i - \mathbf{R}_j|) - C_{ij,\alpha\beta\gamma}^{(3)} P_j^\gamma). \quad (7)$$

Here, E_s is the interaction energy of spherically symmetric ions; E_p , E_q , and E_{pq} are the interaction energies of dipole and quadrupole moments; $E_{\text{self}} = \sum_{i=1}^{N_a} E_i^{\text{ion}}$

is the self-energy of ions; $C_{ij}^{(n)} = \nabla^n \frac{1}{|\mathbf{R}_i - \mathbf{R}_j|}$ is the long-range part of the interactions, which is calculated by the Ewald method; $\Phi_{ij,\alpha\beta\gamma}^{(mn)}(V_i, V_j, |\mathbf{R}_i - \mathbf{R}_j|)$ is the short-range part of the interaction; and $P_i^\alpha (q_i^{\alpha\beta})$ are the dipole (quadrupole) moments of ions, which can be found by minimizing the total energy of the crystal [11].

To find the crystal energy in the disordered phase, we use the virtual-crystal approximation. In this approximation, the short-range part of pair interactions of a virtual ion $\langle B \rangle$ with the other ions (i) is

$$\Phi_{iB}^{II'} = x\Phi_{iB'}^{II'} + (1-x)\Phi_{iB''}^{II'}. \quad (8)$$

The contribution from the virtual ion to the self-energy can be written as

$$E_B^{\text{ion}} = xE_{B'}^{\text{ion}} + (1-x)E_{B''}^{\text{ion}}. \quad (9)$$

The quadrupole and dipole polarizabilities of the virtual ion B are

$$\alpha_B^{d,q} = x\alpha_{B'}^{d,q} + (1-x)\alpha_{B''}^{d,q}. \quad (10)$$

The long-range part of the interaction remains the same as that for the pure components of the solutions.

Let us discuss the phase transition in a $\text{PbZr}_x\text{Ti}_{1-x}\text{O}_3$ solid solution related to ordering of the B cations in the case where $x = 1/2$ and $1/3$. Furthermore, in the effective Hamiltonian (2), we restrict ourselves to interactions within the first three coordination shells. To calculate the effective constants, we find the energies of several structures with different ordering of the titanium ions. For the ordered structures, we use the notation from [12], where an analogous calculation of the energies was performed for the $\text{PbSc}_{1/2}\text{Ta}_{1/2}\text{O}_3$ solid solution. Table 1 lists the configuration motif, the lattice parameters of the ordered structures, the energies per ABO_3 formula unit calculated without and with regard to relaxation of Pb and O ions, and expressions of the energy in terms of the effective constants defined in Eq. (2). The table also gives the energies of mixtures of pure substances PbTiO_3 (PTO) and PbZrO_3 (PZO) for concentrations $x = 1/2$ and $1/3$. It is seen from the Table 1 that at any concentration the most favorable ordered structure considered is the structure with Zr and Ti cations ordered along the body diagonal of the cubic unit cell of the disordered phase. However, without taking the relaxation of Pb and O ions into account, this structure has a somewhat greater energy than the mixture of the pure substances. For concentration $x = 1/2$, the result obtained agrees with calculations performed by other authors [4]. The difference in the energies of the two unrelaxed structures with ordering along the [111] and [100] directions obtained in this study (5.3 mRy) also agrees with the results obtained in other calculations (4.6 and 5.9 mRy [4]).

Since only the degrees of freedom related to positional disorder of B' and B'' atoms are taken into account in the effective Hamiltonian, the effective interaction constants are calculated using the energies of unrelaxed structures. The energy expressed in terms of the effective constants contains a constant energy E_0 , which is independent of the positions of B' and B'' ions and can be taken as the zero of energy. The calculated effective interaction constants are listed in Table 2.

To study the statistical properties of the phase transitions related to the ordering of B cations in the $\text{PbZr}_x\text{Ti}_{1-x}\text{O}_3$ compounds ($x = 1/2, 1/3$), in addition to using the effective Hamiltonian (2), we applied the standard Monte Carlo method [13].

The Monte Carlo procedure consists in the following. As the initial structure, we take one of the ordered structures or the completely disordered structure at a fixed temperature. One Monte Carlo step is sequential running over all lattice sites. For each site (s), one of the nearest neighbors is randomly chosen (s'). If the atoms at sites s and s' are of the same type, then the configuration remains unchanged. If the atoms at sites s and s' differ in type, then we calculate the energy difference between the initial configuration and the configuration in which the atoms in sites s and s' change places:

$$\Delta E^{\text{conf}} = \sum_{i=1}^3 2(m_{B'B'}^{(i)} - m_{B'B''}^{(i)} + \delta) v_i, \quad (11)$$

where $m_{B'B'}^{(i)}$ is the number of i th nearest B' -type neighbors of a B' -type atom, $m_{B'B''}^{(i)}$ is the number of i th nearest B' -type neighbors of a B'' -type atom before the permutation, and $\delta = 1$ if $i = 1$ and $\delta = 0$ if $i = 2, 3$.

The latter condition means that the nearest neighbors change places. The permutation is accepted and the configuration is taken to be new in the following cases: (i) $\Delta E^{\text{conf}} \leq 0$ or (ii) $\Delta E^{\text{conf}} > 0$ if $\xi < \exp[-\Delta E^{\text{conf}}/kT]$, where ξ is a random number and $0 < \xi < 1$.

After each Monte Carlo step, we calculate the energy of the configuration, the short-range order parameter σ , and the long-range order parameter η . The short-range order parameter is defined by [14]

$$\sigma = \left| \frac{n_{B'B''} - n_{B'B''}(\text{disorder})}{n_{B'B''}(\text{order}) - n_{B'B''}(\text{disorder})} \right|, \quad (12)$$

where $n_{B'B''}(\text{disorder}) = \bar{Z}Nx(1-x)$ is the number of $B'B''$ pairs in the completely disordered solid solution, \bar{Z} is the coordination number, N is the number of atoms in the solution, and x is the concentration of atoms of type B' .

For concentration $x = 1/2$, the structures with ordering along the [111], [110], and [100] directions have the lowest energies; therefore, they are of greatest interest. For each of these structures, we calculate the short-range and long-range order parameters.

For different completely ordered structures in the case where $x = 1/2$, the values of $n_{B'B''}(\text{order})$ are

$$\begin{aligned} n_{B'B''}(111) &= 6N, & n_{B'B''}(110) &= 4N, \\ n_{B'B''}(100) &= 2N. \end{aligned}$$

Table 1. Energies of different ordered $\text{PbZr}_x\text{Ti}_{1-x}\text{O}_3$ structures

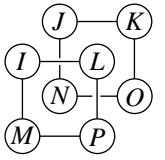
Configuration {IJKL} {MNOP} $B' = +1, B'' = -1$	Lattice parameters ($a_0 = 3.95 \text{ \AA}$)	Calculated energies without regard to the ion self-energy, eV		Expressions of the energy in terms of the effective constants v_i
		without relaxation	with relaxation	
				
$x = 1/2$				
{-1 1 -1 1}	$a = b = c = 2a_0$	-158.128282	-158.253272	$6v_1 + 8v_3 - \mu/2 + E_0$
{1 -1 1 -1}				
$B'B''$ along [111]				
{-1 1 -1 -1}	$a = b = c = 2a_0$	-158.074271	-158.180158	$3v_1 + 6v_2 + 8v_3 - \mu/2 + E_0$
{1 1 1 -1}				
{1 1 1 1}	$a = b = a_0,$	-158.056270	-158.227649	$2v_1 + 8v_2 + 8v_3 - \mu/2 + E_0$
{-1 -1 -1 -1}	$c = 2a_0$			
$B'B''$ along [100]				
{1 -1 1 -1}	$a = b = \sqrt{2}a_0,$	-158.091386	-158.210677	$4v_1 + 8v_2 - \mu/2 + E_0$
{1 -1 1 -1}	$c = a_0$			
$B'B''$ along [110]				
{-1 -1 -1 1}	$a = b = c = 2a_0$	-158.091829	-158.203578	$4v_1 + 6v_2 + 4v_3 - \mu/2 + E_0$
{1 1 1 -1}				
{1 -1 -1 -1}	$a = b = c = 2a_0$	-158.073826	-158.160574	$3v_1 + 8v_2 + 4v_3 - \mu/2 + E_0$
{1 1 1 -1}				
{1 1 1 1}	$a = b = a_0$	-158.012134	-158.900837	$v_1 + 4v_2 + 4v_3 - \mu/2 + E_0$
{1 1 1 1}+	$c = 4a_0$			
{-1 -1 -1 -1}				
{-1 -1 -1 -1}				
1/2PZO + 1/2PTO		-158.157773		
$x = 1/3$				
$B'B''$ along [100]	$a = b = a_0,$ $c = 3a_0$	-159.074277	-159.210991	$(4v_1 + 16v_2 + 16v_3 - 2\mu)/3 + E_0$
$B'B''$ along [111]	$a = b = \sqrt{2}a_0,$ $c = \sqrt{3}a_0$	-159.133164	-159.259862	$4v_1 + 4v_2 + 4v_3 - 2\mu/3 + E_0$
1/3PZO + 2/3PTO		-159.229638		

Table 2. Effective interaction constants (in meV)

v_1	v_2	v_3
-12.22	-1.61	-0.86

For concentration $x = 1/3$, two ordered structures were considered, namely, those with ordering along the [111] and [100] directions. The number of $B'B''$ pairs for the ordered structures in the case of $x = 1/3$ is

$$n_{B'B''}(111) = 4N, \quad n_{B'B''}(100) = 4/3N.$$

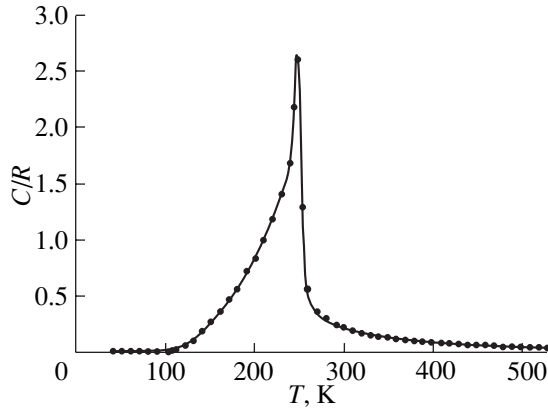


Fig. 1. Temperature dependence of the excess heat capacity related to B -cation ordering in the $\text{PbZr}_{1/2}\text{Ti}_{1/2}\text{O}_3$ solid solution.

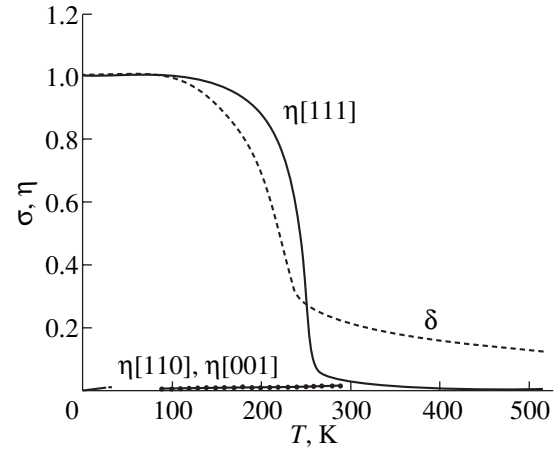


Fig. 2. Temperature dependence of the long-range and short-range order parameters in the $\text{PbZr}_{1/2}\text{Ti}_{1/2}\text{O}_3$ solid solution.

The long-range order parameter for $x = 1/2$ is defined as

$$\eta = \left| \frac{4R_B(B')}{N} - 1 \right|, \quad (13)$$

where $R_B(B')$ is the number of atoms of type B' at their “sites proper.”

For different types of ordering, the B' sites are defined by the following conditions:

$$\exp[i\pi(x + y + z)] = 1, \quad (14a)$$

for ordering along the [111] direction,

$$\exp[i\pi(x + y)] = 1, \quad (14b)$$

for ordering along the [110] direction, and

$$\exp[i\pi(x)] = 1, \quad (14c)$$

for ordering along the [100] direction, where x , y , and z are the site coordinates.

For concentration $x = 1/3$, the long-range order parameter is

$$\eta = \frac{1}{2} \left| \frac{9R_B(B')}{N} - 1 \right|. \quad (15)$$

The B' sites are defined by the following conditions:

$$\cos\left(\frac{2\pi}{3}(x + y + z)\right) = 1, \quad (16a)$$

for ordering along the [111] direction and

$$\cos\left(\frac{2\pi}{3}x\right) = 1, \quad (16b)$$

for ordering along the [100] direction.

We studied lattices $16 \times 16 \times 16$ in size for $x = 1/2$ and $18 \times 18 \times 18$ for $x = 1/3$ with periodic boundary conditions. The first 10 000 steps at each temperature are disregarded and are not included in averaging the quantities E^{conf} , η , and σ . The average values $\langle E^{\text{conf}} \rangle$,

$\langle (E^{\text{conf}})^2 \rangle$, $\langle \eta \rangle$, and $\langle \sigma \rangle$ are calculated in two steps. After $p = 50$ steps, the group averages are calculated:

$$\langle \eta \rangle_g = \frac{1}{p} \sum_{i=1}^p \eta_i, \quad \langle \sigma \rangle_g = \frac{1}{p} \sum_{i=1}^p \sigma_i, \quad (17)$$

$$\langle E^{\text{conf}} \rangle_g = \frac{1}{p} \sum_{i=1}^p E_i^{\text{conf}}, \quad \langle (E^{\text{conf}})^2 \rangle_g = \frac{1}{p} \sum_{i=1}^p (E_i^{\text{conf}})^2.$$

Then, the averaging over $M = 500$ groups is performed:

$$\begin{aligned} \langle \eta \rangle &= \frac{1}{M} \sum_{i=1}^M \langle \eta \rangle_g, & \langle \sigma \rangle &= \frac{1}{M} \sum_{i=1}^M \langle \sigma \rangle_g, \\ \langle E^{\text{conf}} \rangle &= \frac{1}{M} \sum_{i=1}^M \langle E^{\text{conf}} \rangle_g, & (18) \\ \langle (E^{\text{conf}})^2 \rangle &= \frac{1}{M} \sum_{i=1}^M \langle (E^{\text{conf}})^2 \rangle_g. \end{aligned}$$

The heat capacity of the system is defined as $C = \frac{1}{kT^2} (\langle (E^{\text{conf}})^2 \rangle - \langle E^{\text{conf}} \rangle^2)$.

The temperature dependences of the heat capacity and of the short-range and long-range order parameters for $x = 1/2$ are shown in Figs. 1 and 2. At low temperatures, the only stable structure is the structure with the ordering along the [111] direction, which appears both upon heating and cooling. The structures with other ordering types are unstable; this can be seen from Fig. 2. The long-range order parameters of the structures with ordering along the [110] and [100] directions are equal to zero throughout the entire temperature range. The phase transition from the ordered to the disordered state occurs at a temperature of about 250 K. As noted in Section 1, experimental data show that ordering does not occur in the $\text{PbZr}_{1/2}\text{Ti}_{1/2}\text{O}_3$ solid solution.

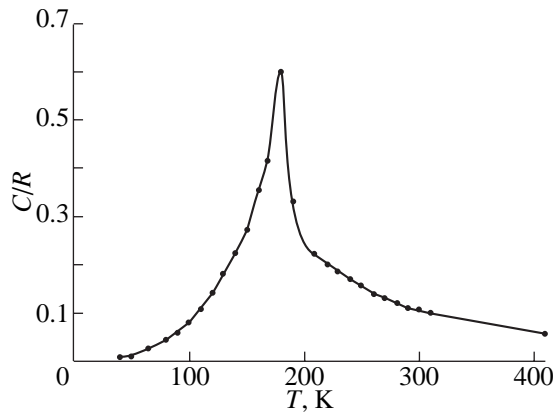


Fig. 3. Same as in Fig. 1 but for the $\text{PbZr}_{1/3}\text{Ti}_{2/3}\text{O}_3$ solid solution.

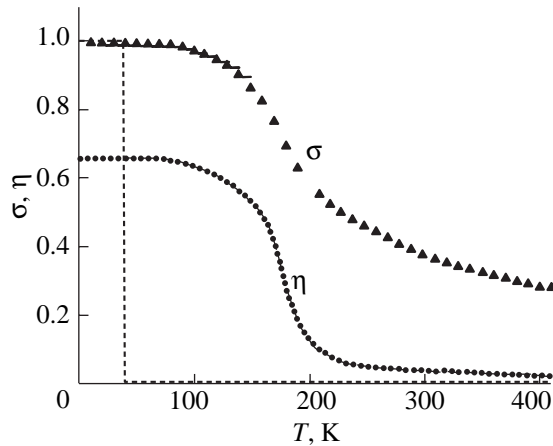


Fig. 4. Temperature dependence of the long-range and short-range order parameters for the $\text{PbZr}_{1/3}\text{Ti}_{2/3}\text{O}_3$ solid solution. Dashed lines show the order parameter for ordering along [111] with a B-cation ratio of 1 : 2, points represent the order parameter for ordering along [111] with a B-cation ratio of 1 : 1 in the heating and cooling modes, and triangles represent the short-range order parameter.

Since the ordering processes in solid solutions, as well as in metal alloys, are diffusive in character, the kinetics of these processes is frozen at the transition temperature obtained, $T = 250$ K, which is much smaller than the melting temperature of PZT ($T_{\text{melt}} \sim 1200$ K); therefore, the phase transition to an ordered state does not occur.

The temperature dependences of the heat capacity and of the short-range and long-range order parameters for concentration $x = 1/3$ are shown in Figs. 3 and 4. The structure with the 1 : 2 ratio and ordering along the [111] direction is metastable for this concentration. If we start the Monte Carlo procedure at a low temperature from this configuration, then the structure collapses with increasing temperature. Part of the solution

becomes ordered along the body diagonal to the Zr/Ti ratio of 1 : 1, and regions of pure Ti appear. With a further increase in temperature (near 180 K), the ordered regions with the 1 : 1 ratio become disordered. In the cooling regime, ordered regions with the 1 : 1 ratio appear at 180 K, and this structure survives down to low temperatures. A peak in the heat capacity is observed to occur at 180 K. There are experimental indications [2] that nanodomains with the ordering of Zr and Ti ions in a ratio of 1 : 1 exist in PZT solid solutions at low temperatures.

3. LATTICE DYNAMICS OF THE DISORDERED AND CERTAIN ORDERED PHASES

The frequency vibration spectrum, high-frequency permittivity, Born effective charges, and elastic moduli of the ordered phases of $\text{PbZr}_x\text{Ti}_{1-x}\text{O}_3$ solid solutions are calculated within the Gordon–Kim model of ionic crystals with regard to deformability and dipole and quadrupole distortions of the electronic density of ions. The corresponding formulas for calculations can be found in [15]. In the case of disordered solid solutions, we calculated the dynamic properties using the virtual-crystal approximation; i.e., in the dynamic matrix, all but the long-range Coulomb contributions are calculated by expanding the interaction energy of a virtual $\langle B \rangle$ ion with the other ions into a Taylor series in small displacements.

First, we discuss the case of disordered solid solutions, which, like the pure components, have a cubic perovskite structure and one molecule per unit cell.

Table 3 lists the calculated lattice cell parameters, high-frequency permittivity, Born effective charges, and elastic moduli for the pure components PbZrO_3 and PbTiO_3 and for solid solutions with concentrations $x = 1/3$, $1/2$, and $2/3$. For comparison, the results of other *ab initio* calculations [16, 17] are also presented. Figure 5 shows the calculated vibration spectrum of the disordered $\text{PbZr}_{1/2}\text{Ti}_{1/2}\text{O}_3$ solid solution for symmetry points and directions in the Brillouin zone, and Table 4 lists the calculated vibration frequencies at the $\Gamma(0, 0, 0)$ and $R(1/2, 1/2, 1/2)$ points for the pure components and for the disordered solutions with concentrations $x = 1/3$, $1/2$, and $2/3$. It is seen from Tables 3 and 4 that the results of our calculations agree (within 10–30%) with the results of other *ab initio* calculations (except for the value of ϵ_∞ for PbTiO_3 obtained in [17]). In solid solutions, as well as in the pure components, there are soft modes in the vibration spectrum. We note that, in addition to a polar vibration mode, our calculations for pure PbTiO_3 predict antiferroelectric lattice instability and that the vibration mode R_{25} , whose eigenvectors correspond to rotation of the TiO_6 octahedron, turns out to be hard. At the same time, in PbZrO_3 , in addition to the ferroelectric and antiferroelectric instabilities, there exists a soft mode R_{25} related to rotation of the ZrO_6 octahedron. All three types of instability exist in a solid

Table 3. Lattice parameter a_0 , permittivity ϵ_∞ , Born effective charge Z , and elastic moduli C_{ij} for crystals $\text{PbZr}_x\text{Ti}_{1-x}\text{O}_3$ in the virtual-crystal approximation

x	$a_0, \text{\AA}$	ϵ_∞	Z_{Pb}	$Z_{\langle B \rangle}$	Z_{O1}	Z_{O3}	$C_{11}, 10^2 \text{ GPa}$	$C_{12}, 10^2 \text{ GPa}$	$C_{44}, 10^2 \text{ GPa}$
0	3.83	4.90	2.78	5.67	-4.93	-1.76	2.58	1.16	1.14
	3.97*	8.24*	3.90**	7.06**	-5.83**	-2.56**			
1/3	3.91	5.21	2.78	5.78	-4.97	-1.79	2.45	0.99	0.96
1/2	3.95	4.87	2.77	5.62	-4.68	-1.86	2.34	0.91	0.90
	3.99***		3.92***	6.47***	-5.28***	-2.54***			
2/3	3.97	4.81	2.77	5.56	-4.53	-1.90	2.42	0.89	0.86
1	4.03	4.50	2.77	5.35	-4.15	-1.98	2.36	0.80	0.78
	4.12*	6.97*	3.92**	5.85**	-4.81**	-2.48**			

* Calculated by the pseudopotential method and the linear-response method [17].

** Calculated by the pseudopotential method and the frozen-phonon method [16].

*** Calculated by the pseudopotential method in the virtual-crystal approximation [6].

solution if the position of a tetravalent cation is occupied by the virtual atom $\langle B \rangle$.

It is seen from Table 1 that, for concentration $x = 1/2$, there are two ordered structures of lowest energies. The structure with the B' and B'' cations ordered along the $[001]$ direction has the $P4/mmm$ symmetry, and the structure with ordering along the $[111]$ direction (the elpasolite structure) has the $Fm3m$ symmetry. For both structures, there are adjustable parameters. In the tetragonal structure, the oxygen ions located between the Zr and Ti ions, as well as the Pb ions, can be displaced along the z axis. In the elpasolite structure, there is a degree of freedom related to “breathing” of the oxygen octahedron. We minimized the total energy with respect to the volume and the free parameters at a constant value of the ratio $c/a = 2.0$ for the tetragonal lattice. For the elpasolite structure, the oxygen octahedron is drawn to the Ti ion by 0.05 \AA . For the tetragonal structure, the

oxygen and lead ions are displaced along the z axis to the Ti ion by 0.11 \AA . The calculated unit cell parameters, high-frequency permittivity, and Born effective charges for these two ordered structures at $x = 1/3$ and $1/2$ are given in Tables 5 and 6; for comparison, the results of other calculations are also presented. It is seen from Tables 5 and 6 that the Born dynamic charges calculated in this study (especially for the lead ion) both in the disordered and in the ordered phases at concentrations $x = 1/2$ and $1/3$ are somewhat smaller than those obtained using the pseudopotential method [18]. It is interesting to note that, in the pure components of a solution, the effective charge of the titanium ion exceeds that of the zirconium ion, whereas for the ordered structures the effective charge of the zirconium ion either is approximately equal to or exceeds that of the titanium ion.

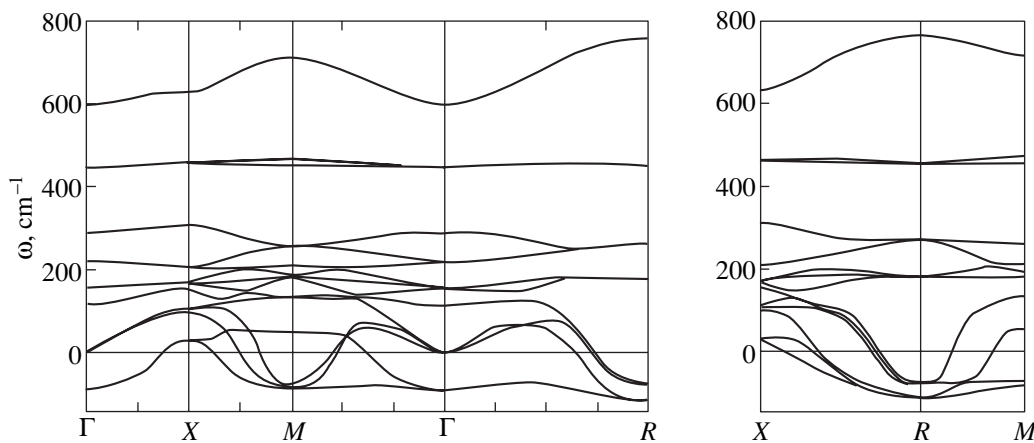

Fig. 5. Phonon spectrum of $\text{PbZr}_{1/2}\text{Ti}_{1/2}\text{O}_3$ calculated in the virtual-crystal approximation.

Table 4. Vibration frequencies (cm^{-1}) for $\text{PbZr}_x\text{Ti}_{1-x}\text{O}_3$ calculated for various concentrations in the virtual-crystal approximation (the mode degeneracy is indicated in parentheses)

x	$q = 0$						
	$TO1(2)$	$LO1$	$T_{2u}(3)$	$TO2(2)$	$LO2$	$TO3(2)$	$LO3$
0	87.3i 144i*	142.0 104*	180.8	236.7 121*	318.9 410*	437.8 497*	616.3 673*
1/3	88.3i	121.6	154.6	222.5	288.7	442.8	608.2
1/2	89.5i	114.7	156.4	219.7	289.6	448.4	600.7
2/3	88.4i	113.3	153.4	218.2	285.5	470.8	611.4
1	91.9i 131i* 140i**	104.9 90*	150.0 30**	214.1 63*	283.5 310*	488.2 486*	609.3 720**
	$q = R$						
	$R_{15}(3)$	$R_{25}(3)$	$R_{15}(3)$	$R_{25}(3)$	$R_{12}(2)$	R_2	
0	110.5i	51.3	177.5	383.0	423.8	718.9	
1/3	119.4i	67.8i	171.8	365.7	438.6	691.2	
1/2	113.3i	77.5i	178.8	342.2	451.6	676.8	
2/3	110.9i	93.6i	181.5	328.5	483.9	677.5	
1	105.0i	113.3i	190.9	299.7	510.8	661.6	

* Calculated by the pseudopotential method and the frozen-phonon method [15].

** Calculated by the pseudopotential method and the linear-response method [16].

Table 5. Lattice parameters, Born effective charges, and permittivity for ordered $\text{PbZr}_{1/2}\text{Ti}_{1/2}\text{O}_3$ solid solutions with different ordering types (for the ordering along [001], the O1 ions lie between Zr and Ti ions, the O2 ions lie in the same plane as the Zr ions, and the O3 ions lie in the same plane as the Ti ions)

Ordering	$a_0, \text{\AA}$	ϵ_∞		Z_{Pb}		Z_{Ti}		Z_{Zr}		Z_{O1}		Z_{O2}		Z_{O3}	
		11	33	xx	zz	xx	zz	xx	zz	xx	zz	xx, yy	zz	xx, yy	zz
Along [111]	$a = 7.88$	4.97	4.97	2.78		5.48		5.77		-1.85	-4.71				
Along [001]	$a = 3.95,$ $c/a = 2.0$	5.01	4.85	2.78	2.84	5.52	6.02	6.10	5.53	-1.79	-4.98	-5.02	-2.12	-5.11,	-1.51
Along [001] (calculation data from [5])	$a = 3.99,$ $c/a = 2.07$	-	-		3.0		5.3		6.0		-4.6		-2.1		-2.1

We calculated the entire lattice vibration spectra in low-energy ordered PZT phases at concentrations $x = 1/3$ and $1/2$. The limiting optical vibration frequencies at $q = 0$ are given in Table 7. For comparison, the table also lists the results of *ab initio* LAPW calculations of limiting frequencies in the $\text{PbZr}_{1/2}\text{Ti}_{1/2}\text{O}_3$ phase ordered along the [111] direction [3]. We see from Table 7 that, for both values of the Zr/Ti ratio in the ordered phases, the crystal lattice is unstable with respect both to the ferroelectric mode ($100.6i$ and $115i \text{ cm}^{-1}$ in the phases $P\bar{3}m1$ and $P4mm$ for $x = 1/3$, respectively, and $87.3i$ and $103.5i \text{ cm}^{-1}$ in the phases $Fm3m$ and $P4/mmm$ for $x = 1/2$, respectively) and to other vibration modes. We

note that, in the ordered $\text{Pb}_2\text{ZrTiO}_6$ with an elpasolite structure, in addition to the ferroelectric soft mode, there is a soft T_{1g} mode that is very close in energy ($87i \text{ cm}^{-1}$) and whose eigenvectors correspond to rotations of the TiO_6 (ZrO_6) octahedrons. Thus, for a Zr/Ti ratio close to $1/2$, we might expect both polar and rotational distortions of the crystal lattice. It is seen from Table 7 that the $\text{Pb}_3\text{ZrTi}_2\text{O}_9$ compound with ordering along the [111] and [001] directions is even more unstable with respect to a ferroelectric mode or other vibration modes that are close in energy. For these values of the Zr/Ti ratio, the pattern of lattice distortions during structural phase transitions can be more complicated.

Table 6. Permittivity and Born effective charges for ordered $\text{PbZr}_{1/3}\text{Ti}_{2/3}\text{O}_3$ solid solutions with different ordering types

Ion	Ordering along [001] (calculation data)				Ordering along [111] (our calculation data)	
	this study		[18]			
	ϵ_{11}	ϵ_{33}	ϵ_{11}	ϵ_{33}	ϵ_{11}	ϵ_{33}
	5.09	5.28	–	–	5.11	5.04
	Z_{xx}	Z_{zz}	Z_{xx}	Z_{zz}	Z_{xx}	Z_{zz}
Pb1	2.88	2.87	3.90	4.04	2.86	2.96
Pb2	2.81	2.92	3.88	3.53	2.93	2.65
Pb3	2.88	2.87	3.90	4.04	2.86	2.96
Ti1	5.50	6.52	6.77	6.65	5.63	5.07
Ti2	5.50	6.52	6.77	6.65	5.63	5.07
Zr	6.09	5.87	6.33	6.69	5.24	5.75
O1	-1.65	-5.32	-2.58	-5.39	-1.69	-5.23
O2	-5.16	-1.62	-5.58	-2.34	-1.57	-5.20
O3	-1.72	-1.62	-2.72	-2.34	-1.57	-5.20
O4	-1.55	-6.09	-2.53	-5.57	-1.65	-4.91
O5	-5.16	-1.62	-5.58	-2.34	-1.79	-4.93
O6	-1.72	-1.62	-2.72	-2.34	-1.65	-4.91
O7	-1.65	-5.32	-2.58	-5.39	-1.79	-4.93
O8	-5.06	-2.17	-5.17	-2.94	-1.65	-4.91
O9	-1.96	-2.17	-2.33	-2.94	-1.65	-4.91

Table 7. Vibration frequencies (cm^{-1}) at $q = 0$ for ordered PZT structures with concentration $x = 1/3$ and $1/2$ (the mode degeneracy is indicated in parentheses)

$\text{Pb}_3\text{ZrTi}_2\text{O}_9$				$\text{Pb}_3\text{ZrTiO}_6$			
ordering along [111], $P\bar{3}m1$ symmetry (our calculation data)		ordering along [001], $P4mm$ symmetry (our calculation data)		ordering along [111], $Fm\bar{3}m$ symmetry (calculation data)		ordering along [001], $P4/mmm$ symmetry (our calculation data)	
				this study	[3]		
100.6i	218.1	115.0i	185.6	87.3i(2)	125i	103.5i	379.7
98.9i	219.2	95.5i	186.6(2)	87.0i(3)		101.8i	398.6
94.6i(2)	237.4	67.5i(2)	195.5	58.2i(3)	16i	28.8(2)	431.9
66.7i	261.8	23.5i	202.0	117.0		75.9	453.3
52.8i	286.5	22.8i	203.9	157.3(3)		82.6	517.5
52.7i	299.6	63.3(2)	227.0	217.5(2)		106.3	625.6
16.9i(2)	332.2	91.4(2)	296.6	226.9(3)	158	119.4	626.1
3.6i	335.3(2)	97.6	319.5	276.5		120.8	
42.3	357.3	102.3	375.9	361.3(2)	326	158.9	
78.3	370.6	116.0	383.4(2)	372.2	357	159.4	
90.3(2)	372.1	138.7(2)	384.8	442.6(2)	538	164.8(2)	
120.9	459.8	141.8	442.9	456.6(2)		190.3	
147.9(2)	489.3(2)	160.3(2)	452.1	608.2		197.5	
156.8	491.8	167.5(2)	551.0	699.7	838	205.9	
207.4	622.2	172.5	628.7			210.6	
211.6	687.5	181.7	650.6			212.9	
214.7(2)	723.7	183.4	666.0			213.8	
215.2						293.3	

4. CONCLUSIONS

Thus, we have written out the effective Hamiltonian and studied the thermodynamic properties of cation ordering in $\text{PbZr}_x\text{Ti}_{1-x}\text{O}_3$ solid solutions using the Monte Carlo method. We have calculated the parameters of the effective Hamiltonian by performing nonempirical total-energy calculations for structures with different types of zirconium and titanium ion ordering. The energies were calculated using the ionic-crystal model with regard to deformability and dipole and quadrupole polarizabilities of the ions. By carrying out Monte Carlo calculations, we determined the cation-ordering phase transition temperatures $T_c \approx 180$ and ≈ 250 K for concentrations $x = 1/3$ and $1/2$, respectively. For the compound under study, these temperatures are much lower than the melting temperature ($T_{\text{melt}} \sim 1200$ K). Due to the alloy ordering being diffusive in character, the ordering kinetics at temperatures close to room temperature is frozen and in reality the phase transition in the ordered phase does not occur, in agreement with experiment.

Using the same ionic-crystal model, we have calculated the high-frequency permittivity, Born dynamic charges, and the lattice vibration spectra for the completely disordered and for the ordered phases of lowest energies. It was found that there are soft vibration modes, including ferroelectric modes, in the lattice vibration spectrum both in the completely disordered and in the ordered phases; moreover, a few soft modes of different symmetry have almost equal energies.

ACKNOWLEDGMENTS

This study was supported by the Russian Foundation for Basic Research (project nos. 03-02-16076, MAS 03-02-06911) and program no. 9 of the Presidium of the Russian Academy of Sciences.

REFERENCES

1. B. Noheda, J. A. Gonzalo, L. E. Cross, R. Guo, S.-E. Park, D. E. Cox, and G. Shirane, *Phys. Rev. B* **61**, 8687 (2000).
2. D. Viehland, *Phys. Rev. B* **52**, 778 (1995).
3. M. Fornari and D. J. Singh, cond-mat/0012126, Vol. 1 (2000).
4. G. Saghi-Szabo and R. E. Cohen, *Ferroelectrics* **194**, 287 (1997).
5. L. Bellaiche and D. Vanderbilt, *Phys. Rev. Lett.* **83**, 1347 (1999).
6. L. Bellaiche and D. Vanderbilt, *Phys. Rev. B* **61**, 7877 (2000).
7. G. Saghi-Szabo, R. E. Cohen, and H. Krakauer, *Phys. Rev. B* **59**, 12771 (1999).
8. H. Fu and O. Gülsereen, *Phys. Rev. B* **66**, 214114 (2002).
9. A. G. Khachatryan, *Theory of Phase Transformations and the Structure of Solid Solutions* (Nauka, Moscow, 1974).
10. O. V. Ivanov and E. G. Maksimov, *Zh. Éksp. Teor. Fiz.* **108**, 1841 (1995) [*JETP* **81**, 1008 (1995)].
11. V. I. Zinenko, N. G. Zamkova, and S. N. Sofronova, *Zh. Éksp. Teor. Fiz.* **123**, 846 (2003) [*JETP* **96**, 747 (2003)].
12. B. P. Burton and R. E. Cohen, *Ferroelectrics* **151**, 331 (1994).
13. N. Metropolis, A. Rosenbluth, M. Rosenbluth, A. Teller, and E. Teller, *J. Chem. Phys.* **21**, 1087 (1953).
14. L. Guttman, *J. Chem. Phys.* **34**, 1024 (1961).
15. N. G. Zamkova, V. I. Zinenko, O. V. Ivanov, E. G. Maksimov, and S. N. Sofronova, *Ferroelectrics* **283**, 49 (2003).
16. W. Zhong, R. D. King-Smith, and D. Vanderbilt, *Phys. Rev. Lett.* **72**, 3618 (1994).
17. P. Ghonsez, E. Cockrayne, U. V. Waghmare, and K. M. Rabe, *Phys. Rev. B* **60**, 836 (1999).
18. L. Bellaiche, J. Padilla, and D. Vanderbilt, cond-mat/9802209, Vol. 1 (1998).

Translated by I. Zvyagin